GEOLOGY | THE GEOLOGICAL SOCIETY OF AMERICA®

https://doi.org/10.1130/G50983.1

Manuscript received 9 December 2022
Revised manuscript received 3 March 2023
Manuscript accepted 27 March 2023

Published online 13 April 2023

© 2023 The Authors. Gold Open Access: This paper is published under the terms of the CC-BY license.

Geochemical significance of lithium and boron isotopic heterogeneity evolving during the crystallization of granitic melts

Xiu-Fang Lei[1,2], Rolf L. Romer[2], Johannes Glodny[2] and Shao-Yong Jiang[1,*]

[1]State Key Laboratory of Geological Processes and Mineral Resources, School of Earth Resources, China University of Geosciences, Wuhan 430074, PR China

[2]Inorganic and Isotope Geochemistry Section 3.1, GFZ German Research Centre for Geosciences, Telegrafenberg, 14473 Potsdam, Germany

ABSTRACT

We present Li and B isotope data for muscovite, biotite, and feldspar + quartz separated from two-mica granite and biotite granite samples from the Huayang-Wulong granite suite (south Qinling, central China). Our data demonstrate systematic differences in the Li and B isotopic compositions among these minerals. Our results indicate that early-crystallizing minerals have lower δ^7Li and δ^{11}B values than the original melt and that residual melts and late magmatic fluids may acquire anomalously high δ^7Li and δ^{11}B values. Furthermore, our data imply that (1) late melts and magmatic fluids do not reflect the composition of their source melt, (2) minerals that crystallized over a large segment of magma evolution may be isotopically zoned, and (3) mineral-selective alteration by late magmatic fluids camouflages the source of the fluid, whose δ^7Li and δ^{11}B values reflect the isotopic compositions of the altered minerals rather than the composition of the remaining rock.

INTRODUCTION

Lithium (Li) and boron (B) are fluid-mobile elements that behave incompatibly during magmatic processes and are expected to show little isotopic fractionation in high-temperature magmatic systems (Tomascak et al., 1999; Romer et al., 2022). The Li isotopic composition of granitic rocks spans a small range, except for highly evolved pegmatites, which have heavier and more variable δ^7Li values (Fig. 1A). The B isotopic composition of different granite types has slightly different ranges (Fig. 1B) and may show systematic regional variations in magmatic arcs, reflecting the different isotopic compositions of mantle and crustal reservoirs involved in the formation of arc granites (Rosner et al., 2003). The B isotopic compositions of S-type granites and pegmatites, however, encompass similar ranges (Fig. 1B). Whole rock samples of differently evolved granite within an individual intrusion show very little variation for both δ^7Li and δ^{11}B (Romer et al., 2022), which is in stark contrast with the large variation in δ^7Li and δ^{11}B values observed for magmatic (and metamorphic) minerals of a given sample (Fig. 1; e.g., Magna et al., 2016; Wolf et al., 2019).

The reason for the small variation at the whole rock scale is well known: large samples average out small-scale heterogeneities (Roddick and Compston, 1977), implying that processes that cause heterogeneity at the small scale may have no effect on the larger scale. The observed δ^7Li and δ^{11}B variations among different mineral phases and within individual crystals have resulted in numerous explanations that may work at different scales. For instance, contrasting δ^7Li among pegmatitic minerals has been interpreted to reflect Li coordination and bond length (Magna et al., 2016), whereas δ^7Li variations on the mineral scale may be due to the faster diffusion of ^{6}Li relative to ^{7}Li (Richter et al., 2003). Similarly, contrasting δ^{11}B among granitic minerals has been ascribed to crystal-melt fractionation and melt-fluid interaction (Fan et al., 2021), whereas core-to-rim variations of δ^{11}B in tourmaline have been interpreted to reflect fluid exsolution followed by loss of the B-rich fluid in open magmatic systems (e.g., Trumbull et al., 2013) and reservoir effects due to Rayleigh fractionation in closed systems (Marschall et al., 2009).

The Li and B isotopic compositions of minerals differ from those of the melts or fluids from which they crystallize (Wunder et al., 2005, 2007). Crystallization of minerals that incorporate Li and B could change the isotopic compositions of these elements in the melt or fluid (Jiang and Palmer, 1998; Marschall et al., 2009). For closed systems, Rayleigh fractionation implies that early- and late-precipitated minerals have different Li and B isotopic compositions, whereas the Li and B isotopic compositions of the bulk rock would not be different from those of the original melt. In open systems, the loss of late melts or fluids has two effects: (1) the residual solid has lower δ^7Li and δ^{11}B values than the original melt, and (2) the lost late melts or fluids have higher δ^7Li and δ^{11}B values than the original melt (e.g., Vlastélic et al., 2011; Trumbull et al., 2013). The magnitudes of the isotopic offsets depend on the fractionation factors and the proportions of Li and B that have been removed from the melt during crystallization. For incompatible elements that strongly partition into the melt or fluid, the difference between early and late melts may be insignificant (Li et al., 2018), whereas for elements that are extracted to some extent from the melt during fractional crystallization, the observed offset may become large, especially for the last batch of melt (e.g., Jiang and Palmer, 1998; Wunder et al., 2005, 2007; Teng et al., 2006).

In this study, we analyze Li and B isotopic compositions for major rock-forming minerals (muscovite, biotite, and feldspar + quartz) from two-mica granite and biotite granite samples in an attempt to reveal the systematic isotopic differences among these minerals and

*shyjiang@cug.edu.cn

CITATION: Lei, X.-F., et al., 2023, Geochemical significance of lithium and boron isotopic heterogeneity evolving during the crystallization of granitic melts: Geology, v. 51, p. 581–585, https://doi.org/10.1130/G50983.1

Downloaded from http://pubs.geoscienceworld.org/gsa/geology/article-pdf/51/6/581/5856287/g50983.1.pdf
by GeoForschungsZentrums Potsdam user

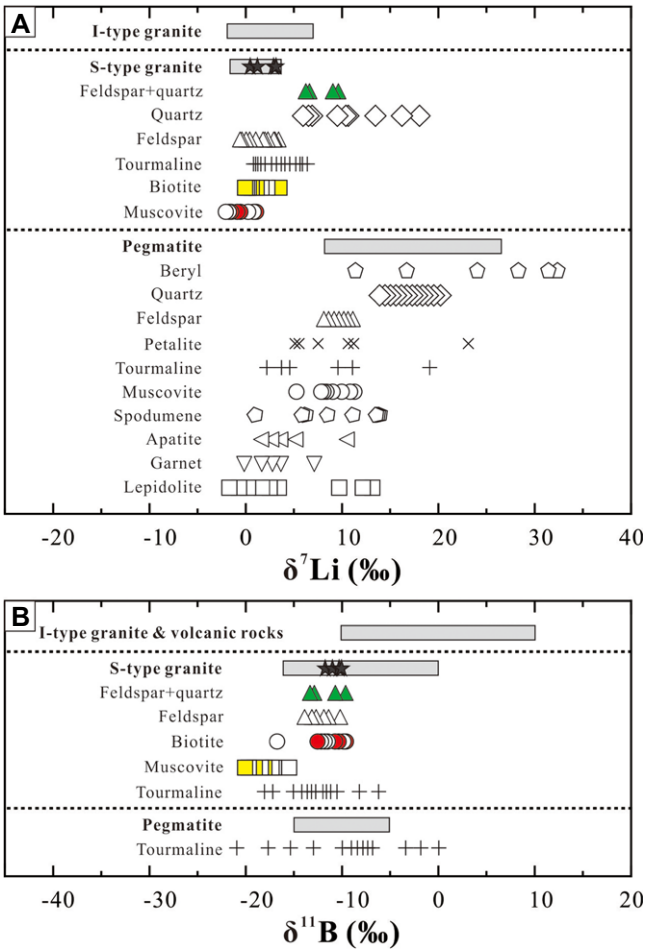

Figure 1. (A) Compilation of δ^7Li values for I-type granites, S-type granites, pegmatites, rock-forming minerals in S-type granites, and various minerals in pegmatites. (B) Compilation of δ^{11}B values for I-type granites and volcanic rocks, S-type granites, pegmatites, rock-forming minerals in S-type granites, and tourmaline in pegmatites. Colored solid symbols—this study; open symbols—mineral data from literature (see below); bar—whole rock data for Li (Teng et al., 2006; Tomascak et al., 2016) and for B (Marschall and Foster, 2018). Sources of mineral δ^7Li data (bulk mineral separates): pegmatites—Teng et al. (2006), Magna et al. (2016), Chen et al. (2020); S-type granites—(Li et al. (2018), Xiang et al. (2020). Sources of mineral δ^{11}B data: tourmaline (*in situ*)—Trumbull et al. (2013); other minerals (bulk mineral separates)—Fan et al. (2021).

corresponding whole rocks and discuss their geologic significance. Our results demonstrate that caution should be taken when using Li and B isotopic compositions of minerals and rocks as petrogenetic source tracers or as process indicators.

SAMPLES AND ANALYTICAL METHODS

The studied samples include three biotite granite samples and one two-mica granite sample from the Huayang-Wulong granite suite (south Qinling, central China) (Qin et al., 2013) (sample location information see Supplemental Material[1]). The granite samples consist of mainly feldspar, quartz, biotite, and muscovite (Table 1). Tourmaline has not been observed in any of the granite samples. Textural features show that muscovite crystallized earlier than biotite in all samples (see the Supplemental Material). An additional sample, a high-temperature altered two-mica granite, shown in Table 1 and the Supplemental Material, is used to highlight the mineralogically controlled effect of post-crystallization alteration. The Li and B isotopic compositions of muscovite, biotite, and feldspar + quartz separates and of the corresponding whole rock samples were determined at GFZ German Research Centre for Geosciences (Potsdam, Germany). For details on analytical procedures, see the Supplemental Material.

RESULTS

All Li and B concentrations and isotopic compositions are shown in Table 1. The reported values represent the weighted mean compositions of the analyzed mineral concentrates, with early-crystallized feldspar and quartz having lower Li and B contents and δ^7Li and δ^{11}B values than later-crystallized feldspar and quartz, which implies that the feldspar + quartz bulk sample is dominated by late-crystallized material (for details, see the Supplemental Material).

Biotite and muscovite are the two main carriers of Li in the biotite-granites and two-mica granite, whereby biotite has higher Li contents (1650–2006 ppm) than muscovite (501–949 ppm). In biotite granites, biotite contributes ~76%–88% to the Li budget, muscovite contributes ~6%–17%, and feldspar + quartz contribute 6%–12% (Table 1). In two-mica granite, biotite and muscovite contribute ~51% and 45%, respectively, to the Li budget (Table 1). The δ^7Li values of muscovite and biotite are –1.9‰ to –0.2‰ and 0.0‰ to 1.5‰, respectively, in biotite granite, and 1.1‰ and 3.4‰, respectively, in two-mica granite (Table 1). The δ^7Li values of muscovite are 1.7‰–2.3‰ lower than those of biotite from the same granites (Fig. 2A). Because biotite is the major Li mineral and dominates the Li budget of the rock, the δ^7Li value of the bulk rock is close to the δ^7Li value of biotite. The feldspar + quartz samples have measured δ^7Li values of 6.3‰–9.6‰ for biotite granites and of 6.7‰ for the two-mica granite sample (Fig. 3). Measured and calculated δ^7Li values (based on mineral proportions and measured Li concentrations and δ^7Li values of the minerals) of bulk rock samples are 0.6‰–3.2‰ and 0.7‰–1.8‰ for biotite granite and 3.2‰ and 2.5‰ for two-mica granite, respectively (Table 1).

Muscovite is the main carrier of B in the biotite granites and the fresh two-mica granite (21–112 ppm), whereas biotite and feldspar + quartz have low contents of B (1.67–3.02 and 1.36–2.61 ppm, respectively) (Table 1). Mass balance indicates that the B budget is dominated by feldspar + quartz for biotite granites and by muscovite and feldspar + quartz for two-mica granite (Table 1). In biotite granites, biotite has δ^{11}B values of –12.7‰ to –9.6‰ and muscovite has values of –18.2‰ to –17.6‰; in two-mica granite, biotite has a δ^{11}B value of –12.0‰ and muscovite has a value of –19.8‰ (Fig. 3; Table 1). Muscovite has systematically lower δ^{11}B values than biotite by 5.6‰–8.0‰ for biotite granites and 7.8‰ for two-mica granite (Fig. 2B; Table 1). Feldspar + quartz have δ^{11}B values of –13.1‰ to –9.6‰ for biotite granites and –12.6‰ for two-mica granite, slightly lower than biotite from the same granites.

DISCUSSION AND IMPLICATIONS

Isotopic fractionation of Li between mineral and liquid strongly depends on temperature and coordination (Wunder et al., 2007; Magna et al., 2016). Lithium has the same coordination in the mineral structures of muscovite and biotite (Magna et al., 2016), and, therefore, muscovite and biotite that crystallize together from the same melt acquire similar δ^7Li values. And yet, our results show muscovite has much lower δ^7Li values than biotite. The crystallization of muscovite and feldspar + quartz removed Li from the melt and shifted δ^7Li of the residual melt to higher values. The ~2‰ offset of δ^7Li between biotite and muscovite (gray band in Fig. 2A) implies that as much as 45%–55% of Li may have been removed from the melt by Rayleigh fractionation before biotite crystallized. As continued crystallization increases the Li contents

[1]Supplemental Material. Samples, analytical methods, alteration effects, and supplemental discussion. Please visit https://doi.org/10.1130/GEOL.S.22344541 to access the supplemental material, and contact editing@geosociety.org with any questions.

Downloaded from http://pubs.geoscienceworld.org/gsa/geology/article-pdf/51/6/581/5856287/g50983.1.pdf
by GeoForschungsZentrums Potsdam user

TABLE 1. Li-B ANALYTICAL RESULTS FOR WHOLE ROCK, BIOTITE, MUSCOVITE, AND FELDSPAR + QUARTZ FROM THE HUAYANG-WULONG GRANITE SUITE OF SOUTH QINLING, CENTRAL CHINA

Sample type	Mineral abundance (%)	Li (ppm)*	δ^7Li ± 2 SE† (‰)	Proportion of whole-rock Li budget§ (%)	Calculated Li (ppm)§	Calculated δ^7Li§ (‰)	B (ppm)#	δ^{11}B ± 2 SE** (‰)	Proportion of whole-rock B budget§ (%)	Calculated B (ppm)§	Calculated δ^{11}B§ (‰)
Fresh two-mica granite (19SQL-97)											
Whole rock		91.1	3.2 ± 0.3		127	2.5	2.41	−11.9 ± 0.2		3.43	−16.1
Biotite	3.20	2006	3.4 ± 0.1	51			3.02	−12.0 ± 0.4	3		
Muscovite	6.00	949	1.1 ± 0.2	45			28	−19.8 ± 0.3	49		
Feldspar + quartz	88	6.76	6.7 ± 0.1	5			1.88	−12.6 ± 0.7	48		
Altered two-mica granite (19SQL-105)											
Whole rock		54.4	1.2 ± 0.3		52	4	6.97	−12.1 ± 0.3		6	−16.8
Biotite	1.00	1722	2.8 ± 0.2	33			47	−10.5 ± 0.2	8		
Muscovite	3.00	881	5.0 ± 0.1	50			112	−19.6 ± 0.2	56		
Feldspar + quartz	94	9.36	3.3 ± 0.2	17			2.29	−10.4 ± 0.4	36		
Biotite granite (19SQL-139)											
Whole rock		106	3.2 ± 0.2		119	1.8	3.91	−11.5 ± 0.2		1.6	−13.8
Biotite	5.50	1895	1.5 ± 0.2	88			1.67	−11.1 ± 0.5	6		
Muscovite	1.30	601	−0.2 ± 0.2	7			21	−17.9 ± 0.6	17		
Feldspar + quartz	91	7.75	8.8 ± 0.3	6			1.36	−13.1 ± 0.8	77		
Biotite granite (19SQL-145)											
Whole rock		107	1.4 ± 0.4		126	1.2	3.41	−10.7 ± 0.2		3.52	−12.9
Biotite	5.50	1752	1.0 ± 0.2	76			2.24	−12.7 ± 0.5	3		
Muscovite	3.00	725	−1.1 ± 0.2	17			35	−18.2 ± 0.3	30		
Feldspar + quartz	90	8.87	9.6 ± 0.2	6			2.61	−10.6 ± 0.3	67		
Biotite granite (19SQL-151)											
Whole rock		100	0.6 ± 0.3		102	0.7	3.03	−10.4 ± 0.4		1.95	−11.1
Biotite	5.00	1650	0.0 ± 0.2	81			1.76	−9.6 ± 0.3	4		
Muscovite	1.30	501	−1.9 ± 0.2	6			28	−17.6 ± 0.3	19		
Feldspar + quartz	92	14	6.3 ± 0.3	12			1.63	−9.6 ± 0.3	77		

*Lithium content was determined using an Element 2XR inductively coupled plasma–mass spectrometer (ICP-MS) (ThermoFisher Scientific).

†Lithium isotopes were analyzed using a Neptune multicollector-ICP-MS (MC-ICP-MS) (ThermoFisher Scientific) operated in standard–sample bracketing mode and using NIST8545 as reference solution. Lithium isotope ratios are expressed in the delta notation relative to measured reference standard NBS951. Samples were analyzed in two or three separate sessions. Each session includes secondary reference materials JG2 and JR2 (Romer et al., 2014) for quality control. The internal precision of repeatedly analyzed sample solution is given as 2 SE (standard error). For analytical details and longtime reproducibility values for reference materials, see text and Romer et al. (2014).

§Whole-rock Li and B budgets were calculated using the measured Li and B concentrations, respectively, of the analyzed minerals biotite, muscovite, and feldspar + quartz and abundances of these minerals. The normative mineral abundances were estimated using the whole-rock compositions of the various samples and the spreadsheet MINSQ (Herrmann and Berry, 2002). Note feldspar and quartz were not separated from each other.

#Boron content was determined on a Neptune MC-ICP-MS (ThermoFisher Scientific) on aliquots of the same sample solution used for isotope analysis.

**Boron isotope ratios were determined using a Neptune MC-ICP-MS (ThermoFisher Scientific) operated in standard–sample bracketing mode and using NBS951 as reference solution. Boron isotope ratios are expressed in the delta notation relative to measured reference standard NIST8545. Samples were analyzed in two or three separate sessions. Each session includes secondary reference materials TB and TS (Govindaraju, 1994; Romer et al., 2014) for quality control. The internal precision of repeatedly analyzed sample solution is given as 2 SE. For analytical details and longtime reproducibility values for reference materials, see text and Romer et al. (2014).

and δ^7Li values of the remaining melt, feldspar + quartz that crystallized throughout the evolution of the melts may have heterogenous Li isotopic compositions, whereby late crystallized feldspar + quartz are expected to have higher Li contents and δ^7Li values (for details, see the Supplemental Material). Fluid inclusions in late quartz cannot account for high δ^7Li values in feldspar + quartz bulk samples (for details, see the Supplemental Material).

The interpretation of δ^{11}B is analogous to the one of δ^7Li, i.e., muscovite crystallized before biotite, and the B budget of feldspar + quartz, which has anomalously high δ^{11}B, is dominated by late-crystallizing feldspar + quartz. There are, however, important differences: (1) muscovite and feldspar + quartz dominate the B budget in two-mica granite, whereas feldspar + quartz dominate the B budget in biotite granite (Table 1); (2) the difference in δ^{11}B between biotite and muscovite is larger than the difference in δ^7Li (Figs. 2 and 3), possibly reflecting that the isotopic fractionation between mineral and melt is larger for B (5‰) than for Li (3‰; Wunder et al., 2005, 2007); and (3) different proportions of B and Li had been extracted from the melt at the onset of biotite crystallization (Fig. 2). As much as 65%–80% of B may have been extracted from the melt at the onset of biotite crystallization (Fig. 2B).

In open systems, the loss of late melts or exsolved fluids would remove liquid with higher δ^7Li and δ^{11}B than the solid (Teng et al., 2006). The actual contrast in δ^7Li and δ^{11}B depends on the fractionation factor and the partitioning behavior of Li and B during fractional crystallization before loss of late melts or fluids (Teng et al., 2006). Mass balance and Rayleigh fractionation imply that the δ^7Li and δ^{11}B values increase during the removal of Li and B by crystallizing magmatic minerals and that early crystallizing minerals have lower δ^7Li and δ^{11}B values than late-crystallizing minerals (Fig. 2). After significant portions of Li and B were incorporated in solid phases, δ^7Li and δ^{11}B values of late melts and exsolved fluids would be markedly higher than those of the initial melt and early crystallized material. For instance, pegmatite, aplite, greisen, and vein-type mineralization may have much higher δ^7Li and δ^{11}B values than the associated granites (Teng et al., 2006; Li et al., 2018; Phelps and Lee, 2022). The contrasting Li and B isotopic compositions of granite and cogenetic pegmatite may lead to the incorrect conclusion that these two kinds of rocks are not related or to the inference of processes (e.g., isotopic fractionation by faster diffusion of ^{6}Li) that are possible but not necessary to explain the data. Similarly, the different isotopic compositions may be incorrectly interpreted to reflect, e.g., (1) the absence of a genetic relation of a pegmatite with local granites, (2) the action of external fluids, or (3) the preferential diffusional loss of the light isotope for systems of unequivocal cogenetic relations, even though the observed difference could be accounted for by Rayleigh fractionation.

Systematic variations in δ^7Li and δ^{11}B have been variably interpreted to reflect Rayleigh fractionation, kinetic fractionation during mineral growth, or diffusion of the lighter isotope (e.g., Marschall et al., 2009; Richter et al., 2003; Phelps and Lee, 2022). For instance, large quartz crystals from pegmatites show variations in δ^7Li

Downloaded from http://pubs.geoscienceworld.org/gsa/geology/article-pdf/51/6/581/5856287/g50983.1.pdf
by GeoForschungsZentrums Potsdam user

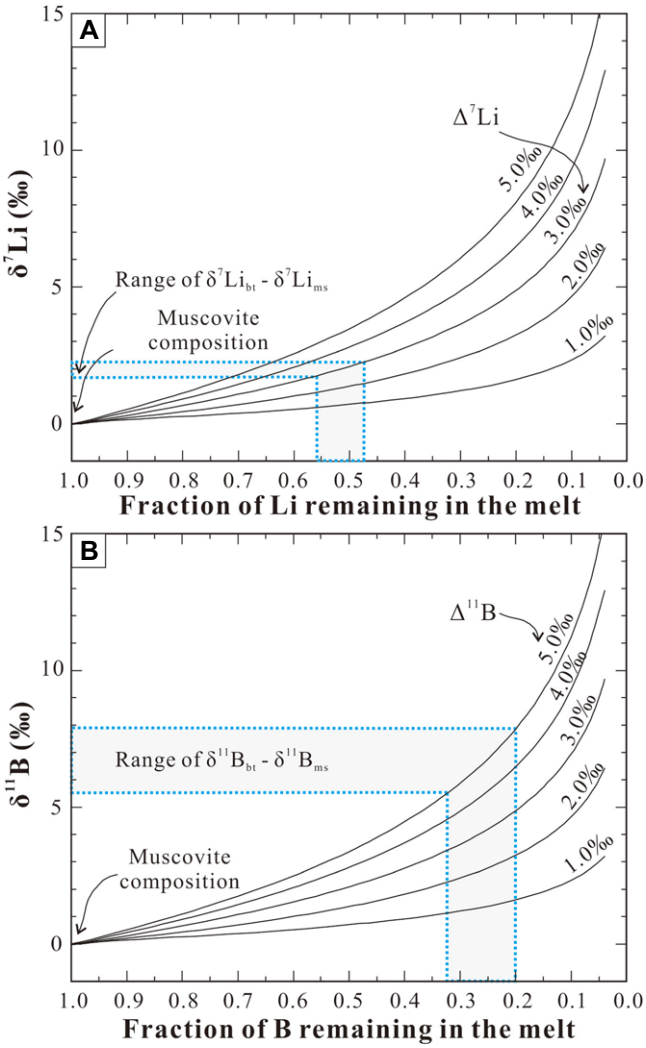

Figure 2. Changes of Li and B isotopic compositions of melt due to Rayleigh fractionation for sampled granites (bt—biotite; ms—muscovite). Curves are calculated for different fractionation factors (Teng et al., 2006). If muscovite, biotite, and feldspar have similar crystal-melt fractionation factors, difference in δ^7Li and δ^{11}B between muscovite and biotite corresponds to change in melt composition when biotite starts to crystallize. Gray band relates differences in δ^7Li and δ^{11}B values with proportions of Li and B remaining in melt.

from core to rim, which reflects Rayleigh fractionation or kinetic effects (Phelps and Lee, 2022). Synthetic tourmaline that crystallized in a closed system and incorporated a significant portion of the available B shows a systematic increase of δ^{11}B values from core to rim due to Rayleigh fractionation (Marschall et al., 2009). Such reservoir effects also explain the contrasting Li and B isotopic compositions of muscovite, biotite, and feldspar + quartz for the analyzed samples. Actually, our data and the above reasoning can be used to predict that any mineral that crystallized over a prolonged period of time during which significant portions of Li and/or B have been extracted from the melt would show core-to-rim isotopic zoning of δ^7Li and/or δ^{11}B. For instance, the heterogeneous Li isotopic composition of zircon with lower δ^7Li values in the core than in the rim, which typically is interpreted to reflect Li diffusion and is used to constrain the cooling history of the magmatic host (Tang et al., 2017; Li and Schmitt, 2021), may alternatively reflect the progressively changing δ^7Li of the evolving host magmas. Our δ^7Li data from muscovite, biotite, and feldspar + quartz imply that the δ^7Li zonation in zircon does not necessarily result from faster diffusion of ^{6}Li but could be easily explained by changes in the δ^7Li composition of the magma, as documented here in the crystallization sequence of major rock-forming minerals.

The range of δ^7Li and δ^{11}B of magmatic minerals also affects how the interaction of the rock with late magmatic and later fluids changes the δ^7Li and δ^{11}B values of the altered rocks. The alteration of magmatic minerals releases Li and B that may be redistributed into secondary minerals or lost to the fluid. Loss of Li and B from the rock may change δ^7Li and δ^{11}B of the altered rock, depending on δ^7Li and δ^{11}B of the altered mineral and the contribution of the lost Li and B to the Li and B budgets of the rock (for details, see the Supplemental Material). In contrast, δ^7Li and δ^{11}B values of the fluid would reflect the composition of the altered minerals (possibly modified by isotopic fractionation if some Li and B were redistributed between secondary minerals and the fluid). Thus, mineral-selective alteration by late magmatic fluids camouflages the source of the fluid as the fluid obtains δ^7Li and δ^{11}B of the altered mineral rather than of the rock. Therefore, contrasting δ^7Li and δ^{11}B isotopic compositions of a granite source and mineral deposits precipitated from late magmatic fluids do not necessarily imply the presence of an additional source of Li and B or rule out a genetic relation between granite and mineral deposit.

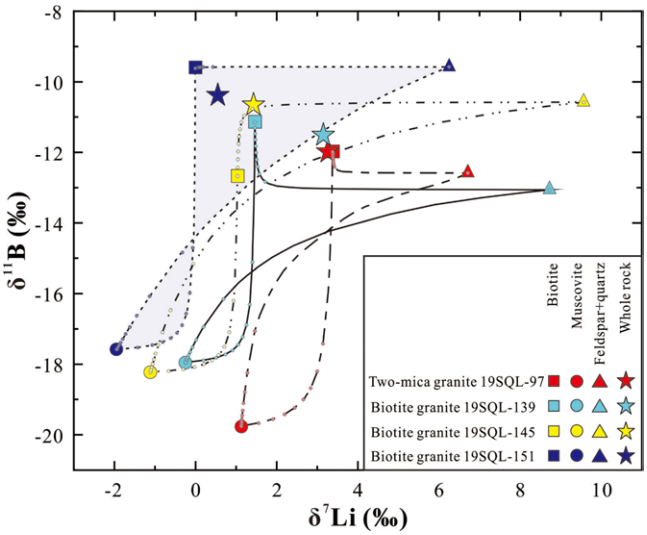

Figure 3. δ^7Li versus δ^{11}B of muscovite, biotite, feldspar + quartz, and bulk rock of four granite samples. Shaded field shows compositional range possible for the three-component system of sample 19SQL-151 (data from Table 1). Limits of fields are calculated as binary mixing curves of mineral end members. Composition of used end members is shown in Table 1. Different line types are used for different samples.

ACKNOWLEDGMENTS

We thank B. Hübner (GFZ) for help in the laboratory. We thank editor Urs Schaltegger, three anonymous reviewers, and Paul Tomascak for thoughtful suggestions. This research was funded by the National Natural Science Foundation of China (grant 42030811). Lei gratefully acknowledges financial support from the China Scholarship Council (grant 202006410082).

REFERENCES CITED

Chen, B., Huang, C., and Zhao, H., 2020, Lithium and Nd isotopic constraints on the origin of Li-poor pegmatite with implications for Li mineralization: Chemical Geology, v. 551, https://doi.org/10.1016/j.chemgeo.2020.119769.

Downloaded from http://pubs.geoscienceworld.org/gsa/geology/article-pdf/51/6/581/5856287/g50983.1.pdf
by GeoForschungsZentrums Potsdam user

Fan, J.J., Wang, Q., Li, J., Wei, G.J., Ma, J.L., Ma, L., Li, Q.W., Jiang, Z.Q., Zhang, L., Wang, Z.L., and Zhang, L., 2021, Boron and molybdenum isotopic fractionation during crustal anatexis: Constraints from the Conadong leucogranites in the Himalayan Block, South Tibet: Geochimica et Cosmochimica Acta, v. 297, p. 120–142, https://doi.org/10.1016/j.gca.2021.01.005.

Govindaraju, K., 1994, Compilation of working values and sample description for 383 geostandard: Geostandards Newsletter, v. 18, p. 1–158, http://doi.org/10.1046/j.1365-2494.1998.53202081.x-i1.

Herrmann, W., and Berry, R.F., 2002, MINSQ—A least squares spreadsheet method for calculating mineral proportions from whole rock major element analyses: Geochemistry: Exploration, Environment, Analysis, v. 2, p. 361–368, https://doi.org/10.1144/1467-787302-010.

Jiang, S.Y., and Palmer, M.R., 1998, Boron isotope systematics of tourmaline from granites and pegmatites: A synthesis: European Journal of Mineralogy, v. 10, p. 1253–1266, https://doi.org/10.1127/ejm/10/6/1253.

Li, J., Huang, X.L., Wei, G.J., Liu, Y., Ma, J.L., Han, L., and He, P.L., 2018, Lithium isotope fractionation during magmatic differentiation and hydrothermal processes in rare-metal granites: Geochimica et Cosmochimica Acta, v. 240, p. 64–79, https://doi.org/10.1016/j.gca.2018.08.021.

Li, S.Q., and Schmitt, A.K., 2021, Lithium distribution and isotopic composition in zircon megacrysts as constraints for their mantle origin and volcanic transfer timescales: Geochimica et Cosmochimica Acta, v. 313, p. 173–194, https://doi.org/10.1016/j.gca.2021.07.032.

Magna, T., Novák, M., Cempírek, J., Janoušek, V., Ullmann, C.V., and Wiechert, U., 2016, Crystallographic control on lithium isotope fractionation in Archean to Cenozoic lithium-cesium-tantalum pegmatites: Geology, v. 44, p. 655–658, https://doi.org/10.1130/G37712.1.

Marschall, H., and Foster, G., eds., 2018, Boron Isotopes: The Fifth Element: Cham, Switzerland, Springer International Publishing, 296 p., https://doi.org/10.1007/978-3-319-64666-4.

Marschall, H.R., Meyer, C., Wunder, B., Ludwig, T., and Heinrich, W., 2009, Experimental boron isotope fractionation between tourmaline and fluid: Confirmation from in situ analyses by secondary ion mass spectrometry and from Rayleigh fractionation modelling: Contributions to Mineralogy and Petrology, v. 158, p. 675–681, https://doi.org/10.1007/s00410-009-0403-8.

Phelps, P.R., and Lee, C.-T.A., 2022, Extreme lithium isotope fractionation in quartz from the Stewart pegmatite: Geochimica et Cosmochimica Acta, v. 336, p. 208–218, https://doi.org/10.1016/j.gca.2022.09.014.

Qin, J.F., Lai, S.C., and Li, Y.F., 2013, Multi-stage granitic magmatism during exhumation of subducted continental lithosphere: Evidence from the Wulong pluton, South Qinling: Gondwana Research, v. 24, p. 1108–1126, https://doi.org/10.1016/j.gr.2013.02.005.

Richter, F.M., Davis, A.M., DePaolo, D.J., and Watson, E.B., 2003, Isotopic fractionation of the major elements of molten basalt by chemical and thermal diffusion: Geochimica et Cosmochimica Acta, v. 67, p. 3905–3923, https://doi.org/10.1016/S0016-7037(03)00174-1.

Roddick, J.C., and Compston, W., 1977, Strontium isotopic equilibration: A solution to a paradox: Earth and Planetary Science Letters, v. 34, p. 238–246, https://doi.org/10.1016/0012-821X(77)90008-5.

Romer, R.L., Meixner, A., and Hahne, K., 2014, Lithium and boron isotopic composition of sedimentary rocks—The role of source history and depositional environment: A 250 Ma record from the Cadomian orogeny to the Variscan orogeny: Gondwana Research, v. 26, p. 1093–1110, https://doi.org/10.1016/j.gr.2013.08.015.

Romer, R.L., Förster, H.J., and Glodny, J., 2022, Role of fractional crystallization, fluid-melt separation, and alteration on the Li and B isotopic composition of a highly evolved composite granite pluton: The case of the Eibenstock granite, Erzgebirge, Germany: Lithos, v. 422–423, https://doi.org/10.1016/j.lithos.2022.106722.

Rosner, M., Erzinger, J., Franz, G., and Trumbull, R.B., 2003, Slab-derived boron isotope signatures in arc volcanic rocks from the Central Andes and evidence for boron isotope fractionation during progressive slab dehydration: Geochemistry, Geophysics, Geosystems, v. 4, 9005, https://doi.org/10.1029/2002GC000438.

Tang, M., Rudnick, R.L., McDonough, W.F., Bose, M., and Goreva, Y., 2017, Multi-mode Li diffusion in natural zircons: Evidence for diffusion in the presence of step-function concentration boundaries: Earth and Planetary Science Letters, v. 474, p. 110–119, https://doi.org/10.1016/j.epsl.2017.06.034.

Teng, F.Z., McDonough, W.F., Rudnick, R.L., Walker, R.J., and Sirbescu, M.-L.C., 2006, Lithium isotopic systematics of granites and pegmatites from the Black Hills, South Dakota: American Mineralogist, v. 91, p. 1488–1498, https://doi.org/10.2138/am.2006.2083.

Tomascak, P.B., Tera, F., Helz, R.T., and Walker, R.J., 1999, The absence of lithium isotope fractionation during basalt differentiation: New measurements by multicollector sector ICP-MS: Geochimica et Cosmochimica Acta, v. 63, p. 907–910, https://doi.org/10.1016/S0016-7037(98)00318-4.

Tomascak, P.B., Magna, T., and Dohmen, R., 2016, Advances in Lithium Isotope Geochemistry: Cham, Switzerland, Springer International Publishing, 195 p., https://doi.org/10.1007/978-3-319-01430-2.

Trumbull, R.B., Beurlen, H., Wiedenbeck, M., and Soares, D.R., 2013, The diversity of B-isotope variations in tourmaline from rare-element pegmatites in the Borborema Province of Brazil: Chemical Geology, v. 352, p. 47–62, https://doi.org/10.1016/j.chemgeo.2013.05.021.

Vlastélic, I., Staudacher, T., Bachèlery, P., Télouk, P., Neuville, D., and Benbakkar, M., 2011, Lithium isotope fractionation during magma degassing: Constraints from silicic differentiates and natural gas condensates from Piton de la Fournaise volcano (Réunion Island): Chemical Geology, v. 284, p. 26–34, https://doi.org/10.1016/j.chemgeo.2011.02.002.

Wolf, M., Romer, R.L., and Glodny, J., 2019, Isotope disequilibrium during partial melting of metasedimentary rocks: Geochimica et Cosmochimica Acta, v. 257, p. 163–183, https://doi.org/10.1016/j.gca.2019.05.008.

Wunder, B., Meixner, A., Romer, R.L., Wirth, R., and Heinrich, W., 2005, The geochemical cycle of boron: Constraints from boron isotope partitioning experiments between mica and fluid: Lithos, v. 84, p. 206–216, https://doi.org/10.1016/j.lithos.2005.02.003.

Wunder, B., Meixner, A., Romer, R.L., Feenstra, A., Schettler, G., and Heinrich, W., 2007, Lithium isotope fractionation between Li-bearing staurolite, Li-mica and aqueous fluids: An experimental study: Chemical Geology, v. 238, p. 277–290, https://doi.org/10.1016/j.chemgeo.2006.12.001.

Xiang, L., Romer, R.L., Glodny, J., Trumbull, R.B., and Wang, R.C., 2020, Li and B isotopic fractionation at the magmatic-hydrothermal transition of highly evolved granites: Lithos, v. 376–377, https://doi.org/10.1016/j.lithos.2020.105753.

Printed in USA

Downloaded from http://pubs.geoscienceworld.org/gsa/geology/article-pdf/51/6/581/5856287/g50983.1.pdf
by GeoForschungsZentrums Potsdam user